Published in Dalton Transactions 2023, 52, 2164; doi: D2DT03984B

C–H Activation in Bimetallic Rhodium Complexes to Afford *N*-Heterocyclic Carbene Pincer Complexes.

Lachlan J. Watson[a] and Anthony F. Hill[a,*]

The pro-ligands 1,8-bis(di-R-phosphinomethyl)-2,3-dihydroperimidine (RH_2Pm, R = phenyl, cyclohexyl) react with $[RhCl(CE)(PPh_3)_2]$ (E = O, S) to afford the bimetallic complexes $[RhCl(CE)(\mu\text{-}RH_2Pm)]_2$ (E = O, S). Upon heating, these species undergo double C–H activation to afford the N-Heterocyclic carbene (NHC) pincer complexes [RhCl(RPm)]. Reduction of $[RhCl(CO)(\mu\text{-}PhH_2Pm)]_2$ with KC_8 results in the bimetallic rhodium(0) complex, $[Rh(\mu\text{-}CO)(PhH_2Pm)]_2$, with a formal Rh–Rh bond and a hydrogen-bonding interaction between rhodium and the central methylene group (C–H···Rh = 2.802 Å). Upon treatment with tritylium, ferrocenium or triphenylcyclopropenium tetrafluoroborates this species undergoes double C–H activation to afford a mononuclear NHC pincer complex salt, $[Rh(CO)(PhPm)]BF_4$. Treatment of $[RhCl(CO)(PhH_2Pm)]_2$ with lithium (trimethylsilyl)acetylide provides another bimetallic species, $[Rh(C{\equiv}CSiMe_3)(CO)(PhH_2Pm)]_2$, however heating this species does not proceed cleanly to the monomeric NHC complex , $[Rh(C{\equiv}CSiMe_3)(CO)(PhPm)]$ which may however be obtained from [RhCl(RPm)] and $LiC{\equiv}CSiMe_3$.

Introduction

The incorporation of *N*-heterocyclic carbene (NHC) donors into pincer ligands continues to provide new organometallic complexes with exciting catalytic[1] and optical[2] properties. Since emerging as isolable species, NHC ligands or their pro-ligands have increasingly competed with traditional phosphine ligands, typically providing increased though variable σ-donation, low π-acidity and bespoke steric profiles.[3,4] The integration of these design features into pincer complexes results in highly tuneable, strongly bound ligands with a high degree of steric control, resulting in a diversity of applications, not least in catalysis.[4–6] To promote more widespread adoption, particularly for industrial applications, factors such as the cost, stability and accessibility of these ligands becomes increasingly important.

We have previously described dihydroperimidine-based pincer pro-ligands RH_2Pm that are available in high yields from a solvent free, one pot reaction of the cheap precursor's paraformaldehyde, 1,8-diaminonapthalene, and a secondary phosphine HPR_2 (R = Ph, Cy, Scheme 1).[7] A single recrystallisation provides air stable and analytically pure pro-ligands. Treatment of these ligands, 1,8-bis(di-R-phosphinomethyl)-2,3-dihydroperimidine (RH_2Pm, R = Ph, Cy), with $[RhCl(PPh_3)_3]$ affords the *N*-heterocyclic carbene complexes [RhCl(RPm)] (R = Ph **1a**, Cy **1b**) *via* dehydrogenative double aminal C–H activation (Scheme 2.).[7]

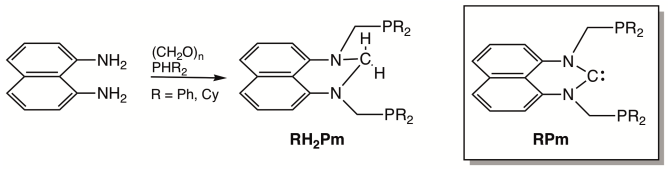

Scheme 1. 1,8-bis(di-R-phosphinomethyl)-2,3-dihydroperimidine ligands (R = phenyl, cyclohexyl).

Expanding the NHC ring from five (more common) to six, projects the amine substituents closer to the coordinated metal, increasing its local steric profile.[8] These perimidinylidene-based NHCs (per-NHCs) also display greater σ-basicity than their five-membered congeners.[9–11] In combination with the bulky phosphine pendant arms and rigid, meridionally enforcing backbone, these species are well positioned as potential catalytic co-ligands, as already demonstrated for **1a** and **1b** which catalyse the selective formylation or methylation of amines using carbon dioxide under remarkably mild conditions.[12] Using the pro-ligand PhH_2Pm as a monodentate donor to the '$RuCl_2Cp$' fragment, Chen and co-workers have also observed catalytic activity, albeit modest, in the transfer hydrogenation of ketones.[13] A related ligand employing a perylene backbone rather than naphthalene fluoresces with a quantum yield of 86%, although this activity is quenched upon addition of $[RhCl(PPh_3)_3]$ and formation of the NHC pincer complex.[14]

The reactions of the pro-ligands (RH_2Pm) with metal centres does not always proceed directly to an NHC pincer ligand (Scheme 1). The resultant bonding mode is dependent on both the phosphine variant (R = Ph or Cy) and the metal precursor. On reaction with

[a] *Research School of Chemistry, The Australian National University, Canberra, ACT 0200, Australia. Email: a.hill@anu.edu.au*

[b] †Electronic Supplementary Information (ESI) available: Synthetic procedures and instrumentation; spectroscopic, computational and crystallographic data.). See DOI: 10.1039/x0xx00000x. CCDC 2222022-2222025.2222038, 2222051 and 22225520 contain the supplementary crystallographic data for this paper, and are available free of charge from the Cambridge Crystallographic Data Centre.

$[RuCl_2(PPh_3)_3]$, the intact phenyl-based ligand (PhH_2Pm) adopts a neutral κ^3-*P,N,P'* coordination mode (Scheme 2) while the more electron rich, bulkier cyclohexyl analogue undergoes double C–H activation.[15] The electron rich species, $[RhCl(PPh_3)_3]$, induces double C–H activation in both ligands (Scheme 2), however for $[IrCl(CO)(PPh_3)_2]$ the reaction halts following single C–H activation without H_2 elimination to provide a one-electron carbon donor CyHPm ligand (Scheme 2).[7] Elimination can sometimes be favoured by utilising hydrogen-accepting co-ligands on the metal precursor such as Cl, H or Ph in order to access the NHC complexes: $[RuClPh(CO)(PhH_2Pm)]$ eliminates benzene upon heating, resulting in the NHC species [RuHCl(CO)(PhPm)].[16] Finally, each phosphine arm in the pro-ligands may act as a monodentate donor to metal fragments such as 'AuCl' or '$RuCl_2(\eta^6\text{-}C_6H_3Me_3)$' in which the metal centres display no interaction with either the ligand backbone or each other.[16]

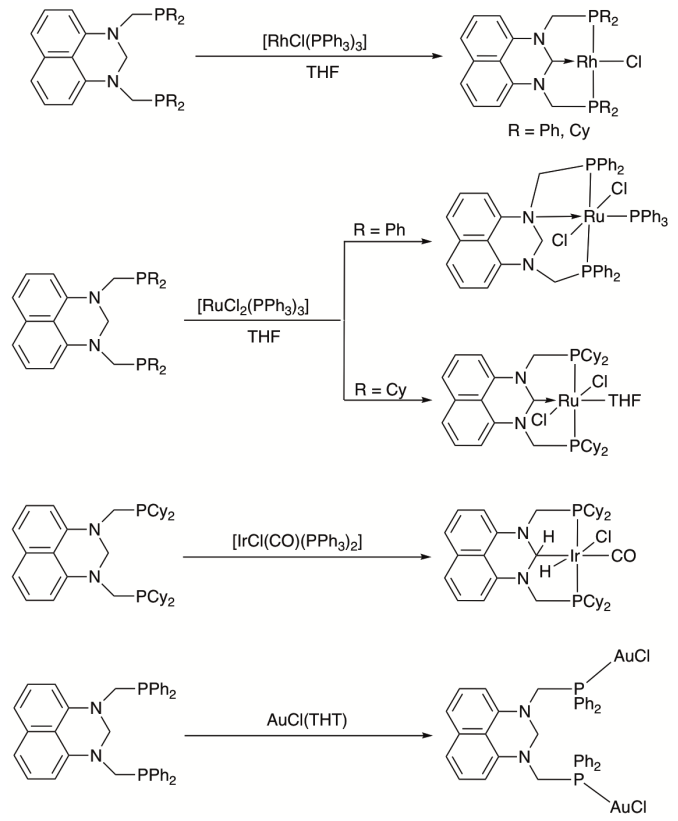

Scheme 2. Known bonding modes of 1,8-bis(di-R-phosphinomethyl)-2,3-dihydroperimidine-derived ligands (R = Ph, Cy; THT = tetrahydrothiophene).

Widespread employment of these RPm pro-ligands requires a reliable installation method, with broader knowledge of the range of binding modes, and the preferences for them. One hurdle is the requirement of a vacant coordination site to effect C-H activation. By analogy to work on similar systems studied by Piers[17] it is likely that the iridium complex above (Scheme 2) is trapped in the *anti*-isomer by a strongly bound CO ligand, preventing isomerism to the *syn* form from which H_2 elimination can occur. The rhodium complex above, $[RhCl(PPh_3)_3]$, undergoes facile double C-H activation despite related systems demonstrating faster activation by iridium than rhodium due in part to enhanced basicity of the metal centre. The formation of iridium carbene complexes via double C–H activation has proven to be particularly facile, not only in the context of PCP pincer carbene installation[18] but even in the absence of chelate-assistance.[19] To further investigate potential installation pathways on complexes with strongly bound, π-accepting co-ligands, the reactions of PhH_2Pm and CyH_2Pm with the rhodium precursors $[RhCl(CE)(PPh_3)_2]$ (E = O S) were investigated. Isolation of other novel complexes and binding modes may provide further insight into installation mechanisms, and ligand interactions (metal-ligand cooperativity) post-installation.

Results and Discussion

Treatment of the dihydroperimidine ligands PhH_2Pm and CyH_2Pm with the rhodium carbonyl and thiocarbonyl complexes $[RhCl(CE)(PPh_3)_2]$ (E = O, S) in dichloromethane rapidly affords the insoluble bimetallic species $[RhCl(CE)(\mu\text{-}RH_2Pm)]_2$ ((E = O, R = Ph **2a**, Cy **2b**; E = S, R = Ph **3a**, Cy **3b**, Scheme 3) in which the RH_2Pm ligands remain intact. Trituration with petroleum spirits and ethanol affords the complexes in analytical purity. Various related dimetallacyclic complexes exist based on both small and complex bidentate phosphines,[20] heteroatomic linkers,[21] and backbones incorporating additional metal centres,[22] which often exhibit similarly poor solubilities.

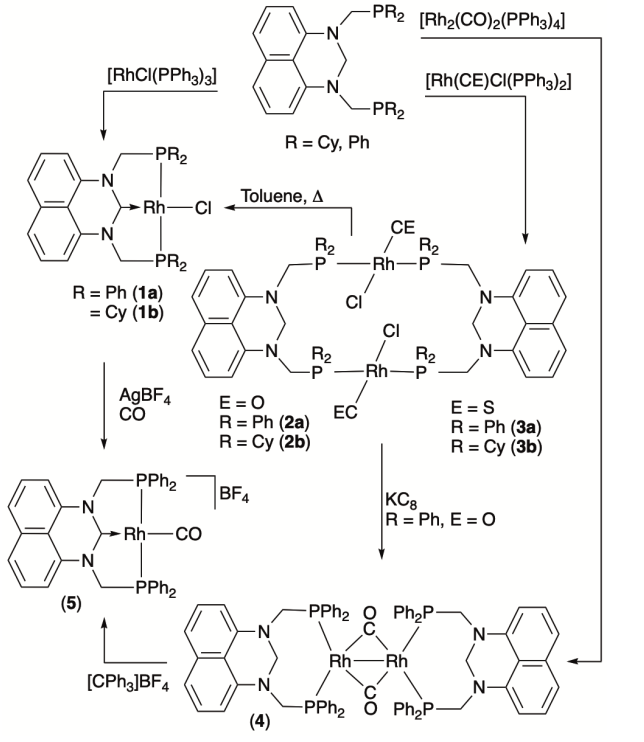

Scheme 3. CH Activation of 1,8-bis(di-R-phosphinomethyl)-2,3-dihydroperimidine ligands (R = phenyl, cyclohexyl).

The minimal impact upon the individual metal coordination spheres is reflected by close similarity of the electronic features of the PhH_2Pm-derived products to those of the monomeric starting materials (Table 1). Increased σ-basicity in the cyclohexyl analogues **2b** and **3b** results in higher electron-density at the metal centre such that the carbonyl infrared stretching frequency (solid state, ATR) of the phenyl complex $[RhCl(CO)(PhH_2Pm)]_2$ (1978 cm^{-1}), is close to that

of the precursor [RhCl(CO)(PPh_3)$_2$] (1970 cm^{-1}), while that of the cyclohexyl analogue occurs at 1954 cm^{-1}. A similar trend is observed for the thiocarbonyl analogues. In each case a strong absorption with rather invariant stretching frequency was also observed at 1591 cm^{-1}, which computational interrogation (ωB97X-D/6-31G*/LANL2DZ) identified as a C=C stretch of the naphthalene backbone (*vide infra*).

The formulation of each complex is reinforced by mass spectrometric (high resolution ESI) and elemental analysis, however, owing to the recalcitrant insolubility of these species, only NMR data of limited utility could be acquired. The phenylphosphine derivatives, **2a** and **3a**, exhibit broad doublets in the $^{31}P\{^1H\}$ NMR spectrum with 124 and 137 Hz $^1J_{RhP}$ couplings, respectively. These couplings are within the range for four coordinate rhodium geometries but may be underestimated due to the broadness of the signals, presumably stemming from libration of the dimers in solution or mutually *syn-anti* isomerism of the Cl–Rh–CO units with respect to each other via rotation about the P–Rh–P axes, recalling Gladysz' molecular gyroscopes [RhX(CO){P(C_6H_4 O$(CH_2)_n$CH=CH$(CH_2)_n$O$C_6H_4)_3$P}] (X = Cl, C≡CPh) for which rotation is fast.[23] A variable temperature NMR study was undertaken for the more soluble species, **3a**, but only revealed modest sharpening of the resonances at 50 °C and thereby a marginally augmented rhodium-phosphorus coupling ($^1J_{RhP}$ = 143 Hz). The signal collapsed to a broad singlet at 0 °C and further cooling resulted in signal loss. For the cyclohexylphosphine complexes, **2b** and **3b**, these solubility issues were dramatically worsened. From $^{31}P\{^1H\}$ NMR spectroscopy, **2b** displays two broad resonances at 42.8 and 34.5 ppm, with the sterically obese phosphines rendering each ^{31}P nucleus distinct. For **3b**, these issues were such that no useful NMR data could be obtained in any common organic solvent (dichloromethane, chloroform, acetone, acetonitrile, water, methanol, ethanol, dimethylsulfoxide, benzene, toluene, tetrahydrofuran, diethyl ether, hexane or cyclohexane).

Table 1. Selected spectroscopic and structural data for the RH_nPm (n = 0,2) Complexes.

Complex	$\nu_{CO/CS}$[a] cm^{-1}	ν_{CC}[a] cm^{-1}	δ_P ppm	$^1J_{RhP}$ Hz	$r_{RhCO/CS}$ Å	$r_{RhC(NHC)}$ Å
Non-NHC Complexes:						
[RhCl(CO)(PPh_3)$_2$]	1970	-	29.5[e]	128	1.810(7)[24]	-
[RhCl(CS)(PPh_3)$_2$]	1301	-	30.9[b]	143	1.787(10)[25]	-
2a	1978	1591	18.5[b]	124	1.824(5)	-
2b	1954	1591	42.8	*d*	1.787(5)	-
			34.5[b]	*d*		
3a	1311	1591	19.6[c]	137	-	-
3b	1283	1591	*d*	*d*	-	-
4	1736	1591	24.0[e]	187	1.968(2)	-
			18.7	201		
6	1986	1590	26.4[f]	131	1.879(3)	-
			15.9			
CH Activated NHC Complexes						
1a	-	1579	22.9[e]	153	-	1.948(4)
1b	-	1580	38.3[e]	148	-	1.930(6)
5	2025	1583	36.9[f]	132	1.907(7)	2.069(7)
7	-	1580	28.6[e]	155		2.000(2)
8	-	1579	29.4[e]	154	-	2.001(2)

[a] Solid state (ATR). [b] Measured in $CDCl_3$. [c] Measured in C_6D_{12}. [d] Insufficiently soluble for data acquisition. [e] Measured in C_6D_6. [f] Measured in CD_2Cl_2.

The two dimeric phenyl complexes [RhCl(CE)(PhH_2Pm)]$_2$ (E = O, S) were sufficiently soluble to allow for recrystallisation and structural characterisation. Complex **2a** is shown (Figure 1), while the thiocarbonyl complex **3a** displays near-identical structural features that are presented in the Supporting Information. Figure 1 demonstrates retention of the square planar geometry about rhodium, with the steric limitations of the PhH_2P ligand only causing a slight deformation of the P-Rh-P angle to 174.58(3)°. Of most interest initially was the enticing 7.169(4) Å separation between the two rhodium atoms, affording space to accommodate either a linker between the metal centres or host small guest molecules. The space-filling inset of Figure 1 suggests a degree of space around each rhodium atom, encouraging further reactivity studies. Cowie[26] observed reaction of [RhCl(CO)(μ-dppm)]$_2$ (dppm = bis(diphenylphosphino)methane) with the activated alkyne dimethylacetylenedicarboxylate (DMAD) to form a new complex with a 5-membered ring devoid of a direct rhodium-rhodium bond, the two metals being bridged by the alkyne and a CO ligand. We have recently observed similar reactivity from a dirhodium carbido complex, [Rh_2(μ-C)(μ-dppm)$_2$] with DMAD to form the first isolable bent carbido complex,[27] however neither DMAD nor methylpropiolate (HC≡CCO_2Me) reacted with **2a** or **3a** at room temperature, and heating in refluxing toluene only yielded unidentifed decomposition products with singlet ^{31}P NMR resonances (*i.e.*, phosphorus no longer bound to rhodium). Other potentially interesting test reactions (CO, H_2, cyclopropenium hexafluorophosphate, diphenylacetylene, $AgPF_6$ in MeCN, tetrabutylammonium fluoride and 1,4-bis(trimethylsilylbutadiyne)) were inconclusive due in part to the extreme insolubility of these complexes: products were often inseparable, and reaction times were slow, with heating affording plethoric mixtures of products. Compounding these issues, the dimeric complexes would themselves undergo self-reaction upon heating.

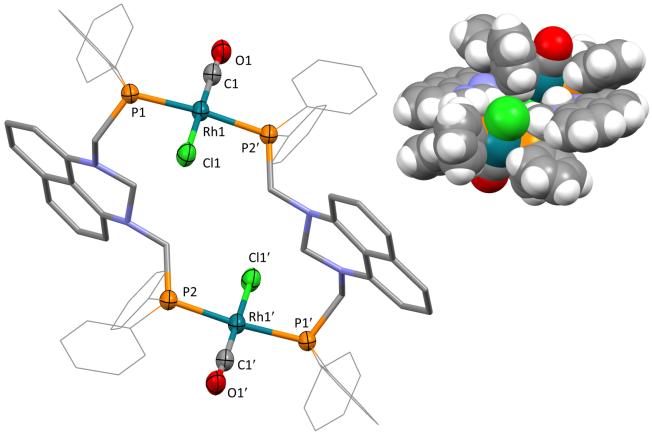

Figure 1. Molecular structure of **2a** (50% displacement ellipsoids, phenyl and napthalene groups simplified, hydrogen atoms omitted for clarity, only one-half of the C_2-symmetric molecule is unique). Space-filling representation inset in the top right. Selected distances [Å] and angles [°]: Rh1–C1 1.824(5), C1–O1 1.126(5), Rh1–Cl1 2.3693(12), Rh1–P1 2.3149(11), Rh1–P2 2.3195(10), Cl1–Rh1–C1 176.19(14), P1–Rh1–P2′ 174.58(3), Rh1–C1–O1 176.9(4).

Heating the dimeric complexes **2a**, **2b** and **3a** in refluxing toluene (Scheme 3), afforded spectroscopically quantitative conversion to the monomeric NHC complexes **1a** and **1b**. In the case of **3b**, $^{31}P\{^1H\}$

NMR spectroscopy exhibited a 2:1 ratio of **1b** and an unknown product (δ_P = 37.7, $^1J_{RhP}$ = 148 Hz). Initially, the iridium complex, [IrHCl(CO)(CyHPm)] (Scheme 2) was presumed to model a plausible intermediate for these reactions, from which elimination of both H_2 and CO might occur. However, conducting sealed-tube NMR experiments, in none of the four reactions (**2a**, **3a** to **1a**; **2b**, **3b** to **1b**, Scheme 2) was H_2 (δ_H = 4.50 in d_8-toluene) observed by ^{1}H NMR spectroscopy. Additionally, while CO dissociation is plausible, dissociation of CS *via* cleavage of a Rh–CS bond seems unlikely due to the strong degree of multiple bond character and high energy of the free molecule, indeed this has rarely been inferred for any chalcocarbonyl complexes.[28] A second possibility of hydride migration to the carbonyl group followed by reductive elimination was considered, however formaldehyde was not observed by ^{1}H NMR spectroscopy, and the intimate mechanism may well be more complicated, involving multi-metallic pathways.

In the hope that a more a reduced species might promote increased reactivity and solubility, **2a** was treated with four equivalents of potassium graphite (KC_8) in benzene, gradually turning red over the course of six hours. Being more soluble than its parent complex, although highly air and moisture sensitive, this species could be isolated by filtration and crystallised from a benzene/diethyl ether mixture and is formulated as the ether solvate of a zerovalent dirhodium complex $[Rh_2(\mu\text{-}CO)_2(PhH_2Pm)_2]\cdot 0.5(Et_2O)$ (**4**, Scheme 3). A pronounced shift of the carbonyl IR absorption from 1978 to 1736 cm^{-1} in this species indicates bridging carbonyl ligands, consistent with a dimeric species rather than cleavage into a monomeric complex. Phosphorus-31 NMR spectroscopy indicates a new species with low symmetry about the rhodium centres presenting distinct phosphorus environments, *viz.* an (**ABRh**)$_2$ system with δ_A = 24.0 and δ_B = 18.7 ($^1J_{BRh} \approx {}^1J_{ARh}$ = 187 Hz). The comparatively large magnitude of the rhodium-phosphorus couplings, indicates a low coordination number at rhodium. These signals arise from distinct chemical environments, rather than phosphorus-phosphorus coupling, as they occur at the same shift regardless of spectrometer frequency (162 or 283 MHz). Phosphorus-phosphorus coupling was not resolved, possibly due to relatively broad signals (36 Hz FWHM).

To ascertain whether these two resonances, which integrate equally, were due to asymmetry in the molecule and not distinct complexes, a 2D ^{31}P–^{1}H HMBC NMR experiment was conducted, roughly adapted from a standard ^{13}C–^{1}H HMBC NMR experiment. This displays a single proton environment coupling to both phosphine signals, confirming they both arise from the one species. Unfortunately, poor solubility and the complex anticipated coupling (ttt) was manifest as only a broad multiplet for the bridging carbonyl resonance (δ_C = 238.5). The sensitivity of this species also prevented the acquisition of useful mass spectrometric data, however a crystal suitable for structural analysis was obtained by slow diffusion of Et_2O into a saturated benzene solution of the sample.

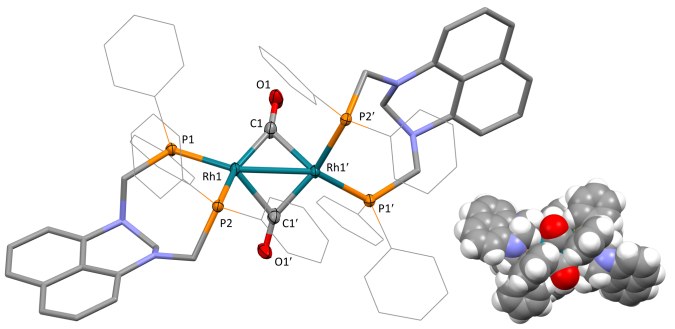

Figure 2. Molecular structure of **4** (50% displacement ellipsoids, naphthalene and phenyl groups simplified for clarity, hydrogen atoms and ether solvate omitted for clarity, only one-half of the C_2-symmetric molecule is unique). Space-filling representation inset bottom right. Selected distances [Å] and angles [°]: Rh1–Rh1′ 2.6066(3), Rh1–C1 1.968(2), Rh1–C1′ 2.052(2), Rh1–P1 2.2987(5), Rh1–P2 2.3106 (5), Rh1–C1–O1 152.26(17), Rh1–C1–Rh1′ 80.83(18), C1–Rh1–C1′ 89.1(1), P1–Rh1–Rh1′–P1′ 73.42(6).

Rather than bridging the two metals as in the precursor, this C_2-symmetric species displays bidentate chelation of the PhH_2Pm ligand. The two ligands are twisted (P1–Rh1–Rh1′–P1′ = 73.42(6)°) with respect to one another, with the two carbonyl ligands raised in a butterfly shape such that the two RhCRh planes are at an angle of 132.3(1)°. The persistence of the d^9-d^9 Rh–Rh bond (2.6066(3) Å) in solution is consistent with the diamagnetic appearance of the NMR spectra obtained.

A small number of complexes of the form $[Rh_2(\mu\text{-}CO)_2(PR_3)_4]$ (PR_3 = PPh_3, $P(O^iPr)_3$, $(PR_3)_2$ = $^iPr_2P(CH_2)_nP^iPr_2$ n = 2,3, DPCB = $Ph_2C_4(PC_6H_3{}^tBu_3)_2$), with more conventional phosphines have been structurally characterised with Rh–Rh bonds ranging from 2.627 to 2.680 Å.[29] Although the PhPm ligand is comparatively bulky, it nevertheless results in the shortest Rh–Rh separation, relative to these other complexes. The torsional angles between related phosphorus donors is somewhat larger for monodentate phosphines (R = O^{i}Pr 101.7°, Ph 101.2°) than for bidentate complexes ($^iPr_2P(CH_2)_nP^iPr_2$: n = 2 80.5, 90.6°; n = 3 79.4°) and **4** (73.4(6)°) with the sterically enormous DPCB example being an outlier at 98.7°. Each of the known complexes features semi-bridging carbonyl ligands (Rh–C–O: 127.0 - 150.7°) as is also observed for **4** (152.26(17)).

Figure 3 suggests a Rh···H interaction in the solid state of (Rh···H–C = 2.802 Å; Rh–H–C = 143°) that is shorter than the sum of the van der Waals radii for the elements (r_{vdW}(Rh) + r_{vdW}(H) = 3.05 Å), and whilst the precision of this measurement is low (riding model placement of the H atom), it would appear that this interaction persists in solution as evident from NMR interrogation. A resonance is apparent downfield at 7.26 ppm in both the ^{1}H-^{13}C{^{1}H} HSQC and ^{1}H–^{1}H COSY NMR spectra, which in the ^{31}P–^{1}H HMBC NMR spectrum shows coupling to both phosphorus nuclei. The resonance for the second aminal hydrogen bound to the same carbon occurs at 4.12 ppm, in the region typical of other complexes of the PhH_2Pm ligand. A two-bond $^2J_{HP}$ path through a direct C–H···Rh interaction is suggested since the resonance for the second geminal proton shows no such coupling while, angular Karplus-type considerations notwithstanding the two $^4J_{HP}$ couplings would be expected to be of comparable magnitudes.

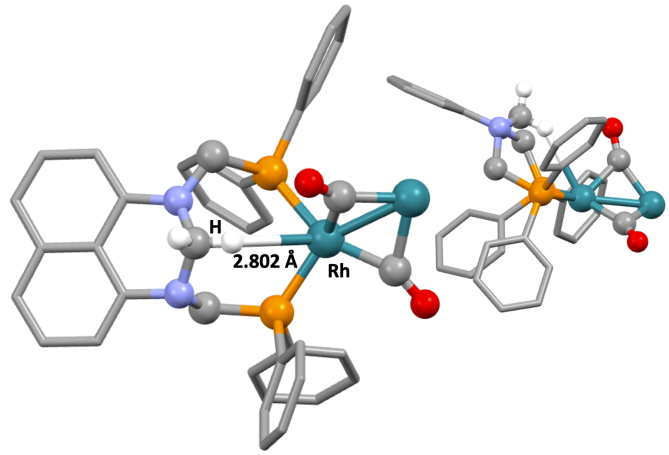

Figure 3. Extract of the molecular structure of **4** highlighting a C–H···Rh interaction.

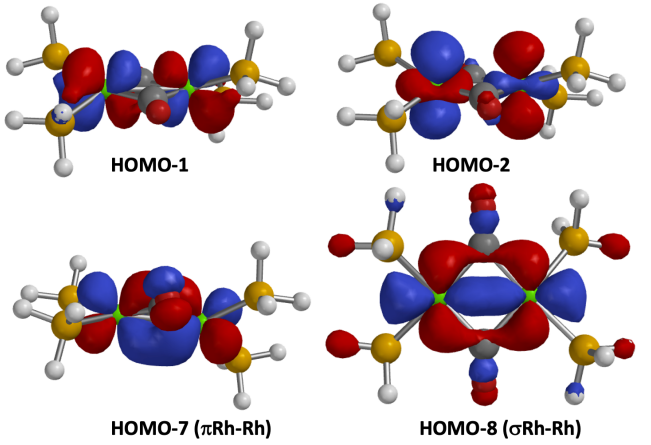

Figure 4. Frontier orbitals of interest for the model complex $[Rh_2(\mu\text{-}CO)_2(PH_3)_4]$ (**4'**).

The nature of the C–H···M interactions for late transition metals has been the subject of much discussion[30] and has been variously described as (a) σ-agostic (3c-2e), (b) pre-agostic (3c-2e), (c) attractive H-bonding (3c-4e) or (d) repulsive anagostic (3c-4e). A tightening of the nomenclature by Brookhart, Green and Parkin in 2007[30b] distinguishes only two forms of M–H–C interactions: agostic; a 3c-2e covalent interaction of hydrogen to both carbon and a metal centre, and anagostic; a largely electrostatic 3c-4e interaction encompassing the previously described pre-agostic and H-bonding descriptions. For C–H bonds interacting with d^8-square planar metals, any one or more of these descriptions might play a role. In the case of the electron-rich high d-occupancy metal centres of (d^9-d^9)-**4**, we are inclined to invoke a considerable contribution from rhodium acting as a hydrogen bond acceptor, *i.e.*, an attractive anagostic rather than pre-agostic interaction for the following reasons. Firstly, the hydrogen atoms of aminals are likely to carry a substantial positive charge. Taking 1,8-dimethyl-2,3-dihydroperimidine as a model, the natural charges on the aminal hydrogens are +0.196 (axial) and +0.237 (equatorial) at the ωB97X-D/6-31G* level of theory. Secondly, the model complex $[Rh_2(\mu\text{-}CO)_2(PH_3)_4]$ (**4'**) which is denuded of steric sterically imposing periphery has, at the same level of theory, *occupied* frontier orbitals of correct symmetry for both hydrogen bond acceptance (HOMO-1) and incipient retrodonation (HOMO-2) to an approaching C–H σ* orbital. Further, interaction with the rhodium centres causes the resonance for the hydrogen atom to shift *downfield* relative to the non-interactive aminal proton, while a conventional agostic interaction would be expected to result in an upfield shift. Finally, the atom-condensed Fukui function derived from natural charges for electrophilic attack at rhodium in **4'** (f^+_{Rh} = 0.12) indicates that the metal centre is primed for electrophilic attack, while that for nucleophilic attack (f^-_{Rh} = 0.07) is at best modest.

It should be noted that f^+_{Rh} is dominated by the impact of ionisation of the HOMO (–6.8 eV). In the case of **4'** this is primarily associated with σ-bonding to the bridging carbonyls and thus orthogonal to the axis of C–H approach, being only very slightly higher in energy than the near degenerate HOMO-1 and HOMO-2 (–7.2 eV). Accordingly, f^+_{Rh} most likely underestimates the propensity of rhodium to enter into either hydrogen bond acceptance or π-retrodonation.

A computational study was employed to further interrogate the electronic interactions of complex **4**, substituting the phenyl substituents for more computationally economical methyl groups in order to obtain a converged structure for $[Rh_2(\mu\text{-}CO)_2(MeH_2Pm)_2]$ (**4^{Me}**) within a cost-effective timeframe. While some of the orbitals (HOMO-2, HOMO-3) become more ligand based, evidence for a rhodium-rhodium interaction is supported by overlap of the two d_{xy} orbitals contributing to the HOMO, and another interaction of the d_{z^2} orbitals in the HOMO-7 (Figure 5). For the simpler model complex **4'**, both σ (HOMO–8) and π (HOMO-7) multi-component Rh–Rh bonding is evident (Figure 4), though higher energy orbitals with Rh–Rh antibonding character reduce the natural Löwdin bond order to 0.651 (2.729 Å), with **4^{Me}** at 0.690 (2.702 Å).

Without the inter-ligand interdigitation of the eight phenyl groups, the C–H···Rh distance in **4^{Me}** is calculated at 2.631Å, in good agreement with the experimentally determined value for **4** of 2.8015(2) Å, suggesting it is genuine and not simple a corollary of Thorpe-Ingold geminal diphenyl compression of the molecule. No covalent Rh–H interaction was, however, observed in the top 30 HOMO's, with none involving any net orbital overlap between the aminal hydrogen and rhodium centres. The natural charge of the hydrogen atom (+0.256) is close to that calculated for the simple dimethyldihydroperimidine noted above. Thus we may conclude that the interaction is primarily that of rhodium acting as a hydrogen bond acceptor. The departure from linearity (C–H–Rh = 143°) is expected to minimise charge transfer contributions,[31] leaving electrostatic factors as the major component.

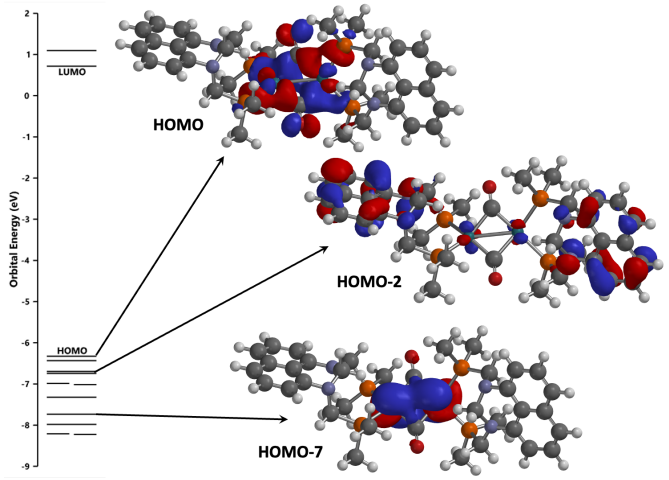

Figure 5. Computational study of the computationally simplified model compound $[Rh(CO)(MeH_2Pm)]_2$ (DFT: ωB97X-D/6-31G*/LANL2Dζ).

One major limitation in the further study of **4** was the difficulty of its synthesis. Excess reducing agent was required for a complete reaction within a reasonable time frame, however over-reduction was common, resulting in a new, unidentified species with a $^{31}P\{^1H\}$ NMR singlet at 24.4 ppm. The lack of rhodium coupling indicates ligand dissociation, and no rhodium containing products could be identified from the resultant mixtures. Other solvents did not improve conversion, as rapid decomposition occurred in THF, and the reaction was prohibitively slow in toluene solutions. Regular monitoring of the reaction by NMR was able to increase the yield to 17%, which remained low enough to inhibit further reactivity studies. Attempts to reduce **3a** in a similar manner met these same issues, and while a new, symmetrical product was observed by NMR (δ_P = 17.2, $^1J_{RhP}$ = 188 Hz), no further data could be obtained. To circumvent the reduction step, PhH_2Pm was added to a benzene solution of $[Rh(CO)(PPh_3)_2]_2$, formed from $[RhH(CO)(PPh_3)_3$ and carbon monoxide,[29d,32,33] and stirred overnight to facilitate ligand replacement, resulting in a 61% yield. Complex **4** appears to have a somewhat fragile construction, as already observed by its decomposition *via* facile over-reduction and oxidation by oxygen. Similarly, reactions of CO_2, CS_2, H_2, dimethylacetylenedicarboxylate, methyl propiolate, PhC≡CPh, 1,4-diphenylbutadiyne, 1,4-bis(trimethylsilyl)butadiyne (*vide infra*), and S_8 with **4** provided complex mixtures of intractable products.

One reaction (Scheme 3) showed remarkable selectivity however: both triphenylcyclopropenium hexafluorophosphate ($[C_3Ph_3]PF_6$) and trityl tetrafluoroborate ($[CPh_3]BF_4$) react rapidly and near quantitatively form the monomeric complexes [Rh(CO)(PhPm)]X (X = PF_6, BF_4, **5**). To ascertain whether the mechanism proceeds *via* hydride abstraction or oxidation of the metal centre, **4** was treated with ferrocenium hexafluorophosphate which resulted in slower, but still clean conversion to **5** in support of an outer-sphere oxidation pathway, after which the cationic rhodium nucleus then eliminates dihydrogen. Complex **5** is more readily synthesised by treatment of **1a** with $AgBF_4$ in acetonitrile, followed by bubbling CO through the solution (Scheme 3).

Conversion of **4** to **5** (Scheme 3) is immediately evidenced by loss of the CH_2 peaks by ^1H NMR, and formation of a symmetrical species with a single doublet in the $^{31}P\{^1H\}$ NMR spectrum at 36.90 ppm, with a 132 Hz $^1J_{RhP}$ coupling indicative of a four or five coordinate rhodium atom. The complexes cationic nature is reflected by its immediate precipitation from the benzene reaction mixtures, high solubility in ethanol, and observation of the BF_4 counter anion by ^{19}F NMR spectroscopy. Indeed, a strong peak is observed in the high-resolution ESI-MS spectrum corresponding to $[M–BF_4]^+$. By $^{13}C\{^1H\}$ NMR spectroscopy, both the NHC carbene and the carbonyl carbon nuclei are observed as doublets of triplets at 209.2 ppm ($^1J_{RhC}$ = 47, $^2J_{PC}$ = 10 Hz), and 195.5 ppm ($^1J_{RhC}$ = 58, $^2J_{PC}$ = 13 Hz), respectively, highlighting a similar degree of *s*-character in these Rh-C interactions.

Formation of the NHC donor is also observed in a shift of the naphthalene backbone CC stretch from 1591 to 1583 cm^{-1}. Table 1 illustrates how formation of an NHC donor, bringing the N*C*N carbon into the plane of the ring, causes a consistent decrease in the stretching frequency of the ring to the extent that this may be diagnostic in future work. Non-interacting perimidine backbones regularly provide IR stretches between 1590 and 1591 cm^{-1} while bound NHC ligands are observed at 1579 to 1583 cm^{-1}. It should be noted that these are not definitive assignments: For the partially activated complex, [IrHCl(CO)(PhHPm)] (Scheme 2), a stretch at 1588 cm^{-1} might be confused with a non-interacting mode as the carbon remains out of the perimidine plane, while the κ^3-*P,N,P'* ruthenium complex, $[RuCl_2(PPh_3)(PhH_2Pm)]$ (Scheme 2, top), has stretches at 1597 and 1584 cm^{-1}.

The cationic nature of **5** results in a shift in the ν_{CO} stretching frequency by IR spectroscopy to 2025 cm^{-1} (ATR) relative to 1978 cm^{-1} in the neutral dimeric species **2a**. This is somewhat higher than observed for other known cationic rhodium(I) species $[Rh(CO)(PhP(CH_2CH_2CH_2PPh_2)_2]HCO_3$ (ν_{CO} = 2004 cm^{-1}),[34] and [Rh(CO)(pigiphos)]OTf (pigiphos = bis{(S)-1-[(R)-2-(diphenylphosphanyl)ferrocenyl]ethyl}-cyclohexylphosphane, ν_{CO} = 2020 cm^{-1}).[35] as well as the NHC-pincer complex $[Rh(CO)\{C(NCHPhPCy_2)_2C_2H_2\}]BF_4$ (1992 cm-1)[36] and $[Rh(CO)\{C(NCH_2PPh_2)_2C_6H_4\}]PF_6$ (1995 cm^{-1}).[37] Furthermore, the non-chelated NHC/phosphine salts $[Rh(CO)\{C(NMe)_2C_2H_2\}(PPh_3)_2]ClO_4$[38a,b] and $[Rh(CO)\{C(NMe)_2C_2H_4\}(PPh_3)_2]ClO_4$[38c] have ν_{CO} = 2001 and 2008 cm^{-1}, respectively. This result is surprising given that perimidine-derived NHC ligands are considered to be more strongly donating than phosphines, imidazolylidene or benzimidazolylidene ligands,[9,10] which should result in a lower stretching frequency. However, it should be noted that for the non-chelated examples, the NHC and rhodium coordination planes are orthogonal,[38b] whilst the pincer framework constrains these near to coplanarity. Despite being less electron rich, this species is still prone to oxidation under ambient conditions and reacts with $CDCl_3$ to afford a mixture of unidentified products.

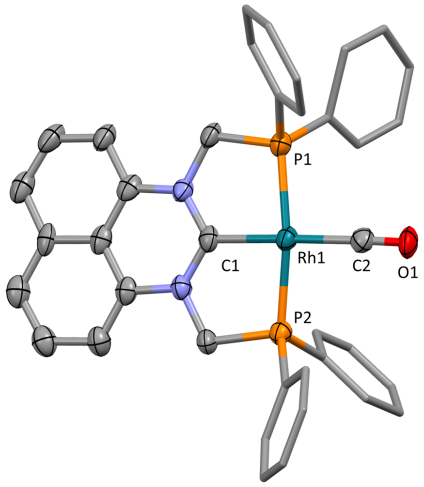

Figure 6. Molecular structure of **5** in a crystal of [**5**]$PF_6 \cdot (C_6H_6)$ (50% displacement ellipsoids, phenyl groups simplified, hydrogen atoms counter-anion and solvent omitted for clarity). Selected distances [Å] and angles [°]: Rh1–C1 2.069(7), Rh1–C2 1.907(7), C2–O1 1.120(9), Rh1–P1 2.2641(19), Rh1–P2 2.2517(18), P1–Rh1–P2 163.17(7), C1–Rh1–C2 173.4(3), Rh1–C2–O1 173.9(7).

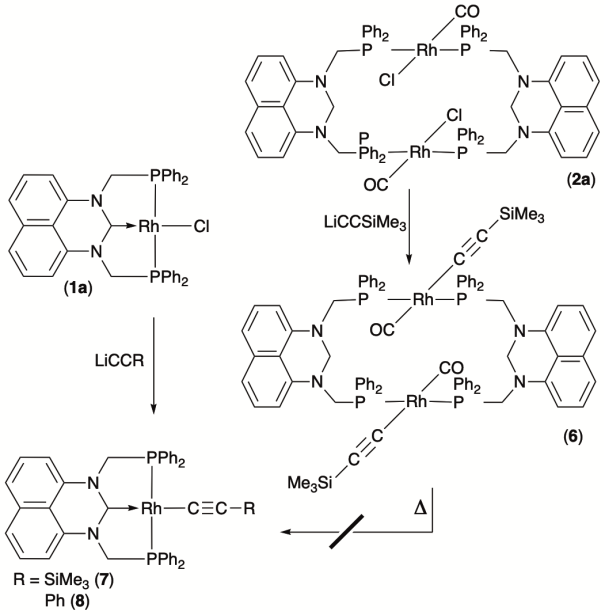

Scheme 4. Mono- and Dinuclear alkynyl complexes.

The decarbonylation of aldehydes remains a valuable tool in natural product synthesis[39] though generally this is achieved stoichiometrically using Wilkinson's 'catalyst' (sic.). This results in formation of $[RhCl(CO)(PPh_3)_2]$ which is unable to re-enter a catalytic cycle due to the prohibitively high temperatures (*ca* 200 °C) required for CO dissociation.[40a] Attempts to develop effective rhodium catalysts have generally relied upon the formation of cationic carbonyl complexes with their attendant increase in CO lability.[40] Thus the cationic complexes $[Rh(dppp)_2]^+$ or $[Rh(CO)_2(dppp)]^+$ (dppp = 1,3-bis(diphenylphosphino)propane) mediate benzaldehyde decarbonylation in refluxing toluene, albeit rather slowly.[40b] Given $[Rh(CO)(dppp)_2]Cl$ has value of ν_{CO} = 1920 cm^{-1},[41] (curiously low for a cationic carbonyl complex), we considered whether complex **5** might be suitable for mediating decarbonylation. Suffice to say, factors that increase CO lability are likely to retard C–H activation and aroyl carbonyl extrusion (retro migratory insertion) and unfortunately this species showed only decomposition in the presence of benzaldehyde at 120 °C.

Though rare, cleavage of the strong (*ca* 670 $kJmol^{-1}$) *(sp)*C–C*(sp)* bond of diynes has been noted previously at both ruthenium[42] and rhodium[43] centres. The inter-rhodium separation in Werner's dirhodabutadiynes $[Rh_2(\mu\text{-}C_4)(L)_2(P^iPr_3)_4]$ of 7.840 Å (L = CO[44a]) and 7.841 Å (L = C=CMe_2[44b]), *cf.* 7.169(4) Å in **2a**) suggested that a similar RhC_4Rh connectivity might be installed beginning with the complexes **2** or **4**. Although **4** does not cleanly react with 1,4-bis(trimethylsilyl)butadiyne, the product envisaged by C-C bond cleavage across the Rh-Rh bond can be accessed by treating **2a** with exactly two equivalents of lithium trimethylsilylacetylide in THF at low temperature to afford the new complex, $[Rh(CO)(C{\equiv}CSiMe_3)(\mu\text{-}PhH_2Pm)]_2$ (**6,** Scheme 4). Excess lithium reagent reacts with **6** to afford further, unidentified products.

Despite the $SiMe_3$ groups projecting tangentially from the metallamacrocycle core, **6** is only marginally more soluble in CH_2Cl_2 than its precursor. This bulk does, however, constrain movement in the core, as do the bulky cyclohexyl complexes **2b** and **3b**, such that the $^{31}P\{^1H\}$ NMR spectrum of **6** displays two distinct, broad resonances at 26.4 and 15.9 ppm. Unlike the cyclohexyl complexes, however, **6** retains sufficient solubility at low temperatures to acquire useful NMR data. At –57 °C, the (**ABX**)$_2$ coupling could be resolved as two doublets of doublets for the diastereotopic phosphorus nuclei, as shown in Figure 7. (CD_2Cl_2: 27.4, 15.9; $^2J_{PP}$ = 289 Hz, $^1J_{RhP}$ = 131 Hz).

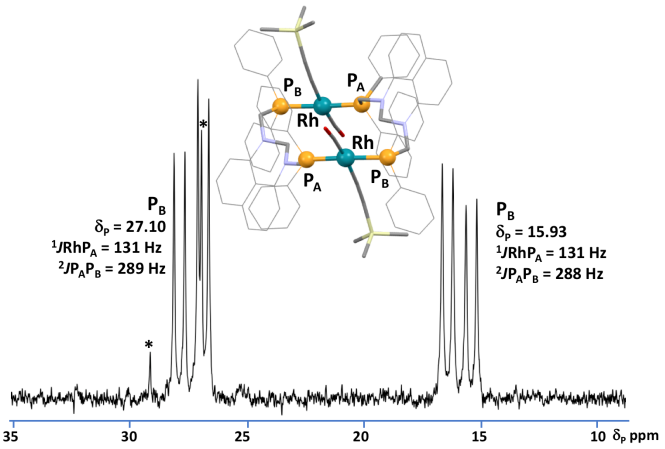

Figure 7. $^{31}P\{^1H\}$ NMR spectrum of **6** (283 MHz, CD_2Cl_2, –57 °C, * = impurity).

The molecular structure of **6** (Figure 8) closely resembles that of its precursor **2a**, with a twisted C_2-symmetric core and parallel approximately square planar rhodium coordination planes (C1–Rh1–C2 169.8(11), P1–Rh1–P2' 170.33(2) Å) despite steric intrusion of the alkynyl groups.

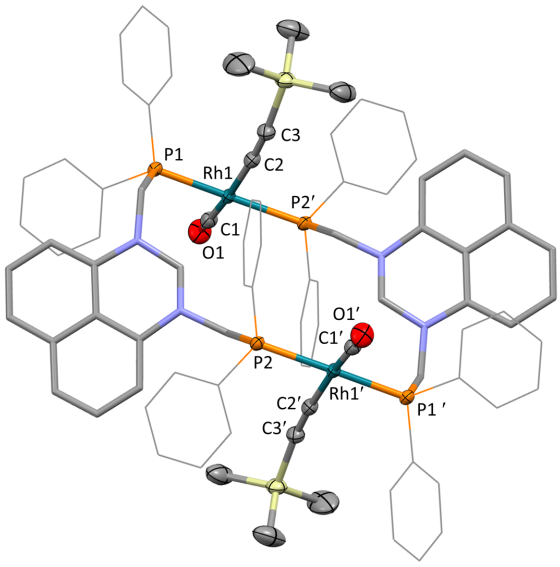

Figure 8. Molecular structure of **6** in a crystal of **6**·(C_6H_6). (50% displacement ellipsoids, naphthalene and phenyl groups simplified, hydrogen atoms and solvent omitted for clarity, only one-half of the C_2-symmetric molecule is unique). Selected distances [Å] and angles [°]: Rh1–C1 1.879(3), Rh1–C2 2.030(3), C2–C3 1.209(4), C1–O1 1.135, Rh1–P1 2.2910(6), Rh1–P2 2.3053(6), O1–C1–Rh1 174.1(3), C1–Rh1–C2 169.8(11), Rh1–C2–C3 169.7(3), P1–Rh1–P2′ 170.33(2).

After three hours heating in toluene under reflux, **6** affords multiple new products by $^{31}P\{^1H\}$ NMR, with three major species (**1**: 21.95, d, $^1J_{RhP}$ = 153 Hz; 2: 27.01, d.br, $^1J_{RhP}$ = 158 Hz, 3: 39.62, d.br, $^1J_{RhP}$ = 156 Hz). The large couplings of these species indicate a four-coordinate rhodium centre, but upon further heating appear to decompose to multiple other products. To ascertain whether one of these species was the NHC based product, [Rh(C≡CSiMe$_3$)(PhPm)] (**7**), its unequivocal synthesis was explored by treatment of **1a** with lithium trimethylsilylacetylide (Scheme 4) at –78 °C. The reaction proceeds smoothly to a new species with a $^{31}P\{^1H\}$ NMR doublet resonance at 28.6 ppm ($^1J_{RhP}$ = 155 Hz), discounting it as a product from the heating of **6**. The analogous reaction of **1a** with lithium phenylacetylide is similarly straightforward, yielding [Rh(C≡CPh)(PhPm)] (**8**). These species are thermally stable but extremely oxygen sensitive, causing the PhPm ligand to dissociate from the metal and providing a multitude of rhodium containing side-products. Treating **1a** with half an equivalent of bis(trimethylsilyl)butadiyne in the presence of [^{n}Bu$_4$N]F ('TBAF') resulted in the formation of a completely insoluble precipitate that defied the acquisition of any useful spectroscopic data and presumably indicates the formation polymeric species rather than the desired bimetallic complex [Rh$_2$(μ-C$_4$)(CO)$_2$(μ-PhH$_2$Pm)$_2$].

The electronic features of **7** and **8** are predictably similar, with $\nu_{C\equiv C}$ stretches at 1995 and 2065 cm^{-1} (CH_2Cl_2), respectively and NHC carbon resonances in near identical positions (δ_C = 218.4 (**7**), 217.4 (**8**)). Signals attributed to C_α (δ_C = 134.0, m) and C_β (135.2, t.br, $^2J_{PC}$ = 5 Hz) of the alkynyl ligand of **7** appeared at somewhat high frequency, their identities being confirmed by ^1H-^{13}C HMBC measurements. While structurally unremarkable, these species illustrate facile, clean substitution reactions on the halide of **1a**, suggesting this fragment could be incorporated into larger structures.

The molecular structures of both **7** (Figure 9) and **8** (see Supporting Information) were crystallographically determined from crystals obtained by standing saturated benzene solutions overnight.

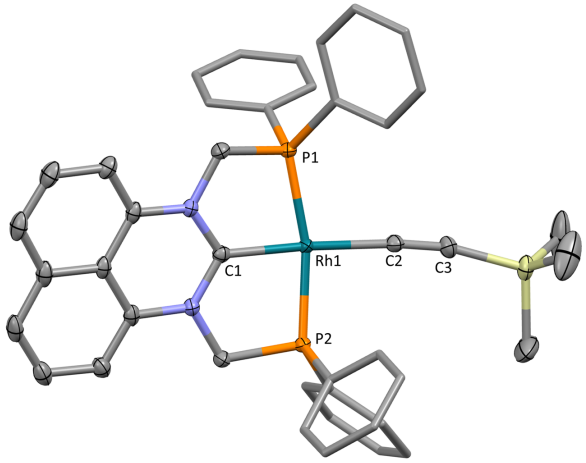

Figure 9. Molecular structure of **7** in a crystal of **7**·(1.5 C_6H_6). (50% displacement ellipsoids, naphthalene and phenyl groups simplified, hydrogen atoms and solvent omitted for clarity). Selected distances [Å] and angles [°]: Rh1–C1 2.000(2), Rh1–C2 2.030(3), C2–C3 1.218(3), Rh1–P1 2.2209(5), Rh1–P2 2.2171(5), C1–Rh1–C2 173.04(8), Rh1–C2–C3 172.7(2), P1–Rh1–P2 165.88(2).

There is clear retention of square planar geometry at rhodium (C1–Rh1–C2 = 173.04(8)°), although the phosphines are pulled back slightly from the alkyne substituent in a similar manner to **5** (P1–Rh1–P2 = 165.88(2)°) reflecting the constraints of chelation. The slight bending of the alkyne (Rh1–C2–C3 = 172.7(2)°) is not uncommon in metal-alkynyl complexes, with an average angle of 174.4 in over 6000 structures archived in the CCDC. Curiously, despite significant electronic differences between the cationic complex **5** bearing a π–accepting CO ligand and neutral **7** with an alkynyl substituent, the NHC carbon-rhodium bond lengths are only minutely affected (Rh1–C1: **5** = 2.069(7), **7** = 2.000(2) Å).

Conclusions

The RH$_n$Pm (n = 0, 1, 2) family represents an economically and expediently accessible group of ligands for future fundamental, optical and catalytic applications, with the caveat of its capricious installation onto various metal centres. Activation of the CH_2 core to afford the desired NHC pincer complexes requires sufficiently electron rich metal centres capable of double C–H activation. This study adds to previous work by illustrating how the bimetallic complexes **2a**-**3b** formed can be heated to afford the NHC complexes **1a** and **1b** upon loss of H_2 and a CE (E = O, S) ligand, although the mechanism of this conversion remains unknown. Additionally, reduction of **1a** affords a new bimetallic Rh(0) complex (**4**) with a metal-metal bond, oxidation of which, with trityl or ferrocenium salts, triggers double C–H activation, presenting a new cationic NHC complex of rhodium (**5**) with a CO ligand. The bimetallic complexes **2a**-**3b** may represent species of interest in their own right, however their recalcitrant insolubility prohibits many further investigations. Heating of a different bimetallic complex, **6,** with alkynyl substituents

does not successfully provide the NHC complex **7**, however, indicating that heat promoted C–H activation may not be functional group tolerant for late-stage installation of these pincer ligands. However, the treatment of **1a** with $AgBF_4$ and CO, or with lithium acetylides does illustrate the ease of structural modification of these complexes *after* ligand installation.

Acknowledgements

We gratefully acknowledge the Australian Research Council (DP190100723 and DP200101222) for funding. LJW gratefully acknowledges the award of a Westpac Future Leaders Scholarship.

Conflicts of Interest

There are no conflicts to declare.

Experimental

General experimental details and instrumentation, synthetic methods, spectroscopic data, selected spectra, cartesian coordinates and computational details are provided in the accompanying Electronic Supporting Information.

Author Contributions

LJW was responsible for the design and execution of the experimental research, the acquisition and critical analysis of the characterisation data and compilation of the original draft. AFH was responsible for funding acquisition, project conceptualisation and administration, validation and refinements to the manuscript.

Notes and references

1 I. Ortega-Lepe, A. Rossin, P. Sánchez, L. L. Santos, N. Rendón, E. Álvarez, J. López-Serrano and A. Suárez, *Inorg. Chem.*, 2021, **60**, 18490–18502.
2 J. Liu, T. L. Lam, M. K. Sit, Q. Wan, C. Yang, G. Cheng and C. M. Che, *J. Mat. Chem. C*, 2022, **10**, 10271–10283.
3 M. N. Hopkinson, C. Richter, M. Schedler and F. Glorius, *Nature*, 2014, **510**, 485–496.
4 R. E. Andrew, L. González-Sebastián and A. B. Chaplin, *Dalton Trans.*, 2016, **45**, 1299–1305.
5 R. Taakili and Y. Canac, *Molecules,* 2020, **25**, 2231–2249.
6 Y. Wang, B. Zhang and S. Guo, *Eur. J. Inorg. Chem.*, 2021, 188–204.
7 A. F. Hill and C. M. A. McQueen, *Organometallics*, 2012, **31**, 8051–8054.
8 A. F. Hill, C. Ma, C. M. A. McQueen and J. S. Ward, *Dalton Trans.*, 2018, **47**, 1577–1587.
9 P. Bazinet, G. P. A. Yap and D. S. Richeson, *J. Am. Chem. Soc.*, 2003, **125**, 13314–13315.
10 P. Bazinet, T. G. Ong, J. S. O'Brien, N. Lavoie, E. Bell, G. P. A. Yap, I. Korobkov and D. S. Richeson, *Organometallics*, 2007, **26**, 2885–2895.
11 G. D. Frey, E. Herdtweck and W. A. Herrmann, *J. Organomet. Chem.*, 2006, **691**, 2465–2478.
12 R. H. Lam, C. M. A. McQueen, I. Pernik, R. T. McBurney, A. F. Hill and B. A. Messerle, *Green Chem.*, 2019, **21**, 538–549.
13 Q. Fu, L. Zhang, T. Yi, M. Zou, X. Wang, H. Fu, R. Li and H. Chen, *Inorg. Chem. Commun.*, 2013, **38**, 28–32.
14 S. Langbein, H. Wadepohl and L. H. Gade, *Organometallics*, 2016, **35**, 809–815.
15 A. F. Hill and C. M. A. McQueen, *Organometallics*, 2014, **33**, 1909–1912.
16 C. M. A. McQueen, A. F. Hill, C. Ma and J. S. Ward, *Dalton Trans.*, 2015, **44**, 20376–20385.
17 J. R. Logan, W. R. Piers, J. Borau-Garcia and. D. M. Spasyuk, *Organometallics*, 2016, **35**, 1279-1286.
18 (a) C. J. Moulton and B. L. Shaw, *J. Chem. Soc., Dalton Trans.*, 1976, 1020-1024. (b) C. Crocker, H. D. Empsall, R. J. Errington, E. M. Hyde, W. S. McDonald, R. Markham, M. C. Norton, B. L. Shaw and B. Weeks, *J. Chem. Soc., Dalton Trans.*, 1982, 1217-1224. (c) H. D. Empsall, E. M. Hyde, R. Markham, W. S. McDonald, M. C. Norton, B. L. Shaw and Brian Weeks, *J. Chem. Soc., Chem. Commun.,* 1977, 589-590. (d) For a recent review see R. A. Manzano and R. D. Young, *Coord. Chem. Rev.*, 2021, **449**, 214215.
19 (a) M. T. Whited and R. H. Grubbs, *Acc. Chem. Res.,* 2009, **42**, 1607-1616. (b) O. Boutry, E. Gutiérrez, A. Monge, M. C. Nicasio, P. J. Pérez and E. Carmona, *J. Am. Chem. Soc.*, 1992, **114**, 7288-7290. (c) D.-H. Lee, J. Chen, J. W. Faller and R. H. Crabtree, *J. Chem. Soc., Chem. Commun.*, 2001, 213-214. (d) E. Carmona, M. Paneque, L. L. Santos and V. Salazar, *Coord. Chem. Rev.*, 2005, **249**, 1729-1735.
20 (a) J. R. Dilworth, Y. Zheng and D. V. Griffiths, *Dalton Trans.*, 1999, 1877. (b) F. C. March, R. Mason, K. M. Thomas and B. L. Shaw, *J. Chem. Soc., Chem. Commun.*, 1975, 584–585. (c) M. S. Balakrishna, D. Suresh, P. Kumar and J. T. Mague, *J. Organomet. Chem.*, 2011, **696**, 3616-3622. (d) M. Cowie and S. Dwight, *Inorg. Chem.*, 1980, **19**, 2500-2507. (e) F. Xu, Q. Li, X. Zeng, X. Leng and Z.-Z. Zhang, *Organometallics*, 2002, **21**, 4894–4896. (f) A. Obenhuber and K. Ruhland, *Organometallics*, 2011, **30**, 171–186. (g) J. M. López-Valbuena, E. C. Escudero-Adan, J. Benet-Buchholz, Z. Freixa and P. W. N M van Leeuwen, *Dalton Trans.*, 2010, **39**, 8560–8574. (h) M. F. M. Al-Dulaymmi, D. L. Hughes and R. L. Richards, *J. Organomet. Chem.*, 1992, **424**, 79–86. (i) N. Janjic, G. Peli, L. Garlaschelli, A. Sironi and P. Macchi, *Cryst. Growth Des.*, 2008, **8**, 854-862. (j) M. F. Haddow, A. J. Middleton, A. G. Orpen, P. G. Pringle and R. Papp, *Dalton Trans.*, 2009, 202-209.
21 (a) A. L. Balch, A. L. Fossett, M. M. Olmstead, D. E. Oram and P. E. J. Reedy, *J. Organomet. Chem*, 1993, **455**, 107–113. (b) A. L. Balch, M. Ghedini, D. E. Oram and P. E. Reedy, *Inorg. Chem.*, 1987, **26**, 1223–1229. (c) I. Bartz, J. Grobe, K. Lutke-Brochtrup, B. Krebs, J. Kuchinke and L. Mechtild, *Z. Anorg. Allg. Chem.*, 2001, **627**, 1334–1346. (d) C. M. Thomas, R. Mafua, B. Therrien, E. Rusanov, H. Stœckli-Evans and G. Süss-Fink, *Chem. Eur. J.*, 2002, **8**, 3343–3352. (e) A. D. Burrows, M. F. Mahon, M. T. Palmer and M. Varrone, *Inorg. Chem.*, 2002, **41**, 1695–1697. (f) N. W. Alcock, J. M. Brown and J. C. Jeffery, *J. Chem. Soc., Dalton Trans.*, 1977, 888. (g) X. Liu, A. H. Eisenberg, C. L. Stern and C. A. Mirkin, *Inorg. Chem.*, 2001, **40**, 2940–2941. (h) M. R. J. Elsegood, A. J. Lake, R. J. Mortimer, M. B. Smith and G. W. Weaver, *J. Organomet. Chem.*, 2008, **693**, 2317–2326. (i) M. R. J. Elsegood, A. J. Lake, R. J. Mortimer, M. B. Smith and G. W. Weaver, *J. Organomet. Chem.*, 2008, **693**, 2317–2326.
22 (a) Q. Folashade Mokuolu, P. A. Duckmanton, P. B. Hitchcock, C. Wilson, A. J. Blake, L. Shukla and J. B. Love, *J. Chem. Soc., Dalton Trans.*, 2004, **4**, 1960–1970. (b) T. Rüffer, M. Ohashi, A. Shima, H. Mizomoto, Y. Kaneda and K. Mashima, *J. Am. Chem. Soc.*, 2004, **126**, 12244–12245. (c) T. W. Graham, A. Llamazares, R. McDonald and M. Cowie, *Organometallics*, 1999, **18**, 3502–3510. (d) C. G. Oliveri, N. C. Gianneschi, S. B.

T. Nguyen, C. A. Mirkin, C. L. Stern, Z. Wawrzak and M. Pink, *J. Am. Chem. Soc.*, 2006, **128**, 16286–16296.
23 L. Wang, F. Hampel and J. A. Gladysz, *Angew. Chem., Int. Ed.,* 2006, **45**, 4372-4375.
24 A. Ceriotti, G. Ciani and A. Sironi, *J. Org. Chem.*, 1983, **247**, 345–350.
25 J. L. De Boer, D. Rogers, A. C. Skapski and P. G. H. Troughton, *Chem. Commun.*, 1966, 756–757.
26 M. Cowie and T. G. Southern, *Inorg. Chem.*, 1982, 246–253.
27 (a) H. J. Barnett and A. F. Hill, *Angew. Chem., Int. Ed.*, 2020, **59**, 4274–4277. (b) H. J. Barnett and A. F. Hill, *Chem. Commun.*, 2020, **56**, 12593-12596
28 Reviews: (a) I. S. Butler, *Acc. Chem. Res.* 1977, **10**, 359-365; (b) P. V. Broadhurst, *Polyhedron* 1985, **4**, 1801-1846; (c) I. S. Butler, *Pure Appl. Chem.* 1988, **60**, 1241-1244; (d) W. Petz, *Coord. Chem. Rev.* 2008, **252**, 1689-1733. (e) B. J. Frogley, A. F. Hill and L. J. Watson, *Chem. Eur. J.*, 2020, **26**, 12706-12716.
29 (a) R. R. Burch, E. L. Muetterties, A. J. Schultz, E. G. Gebert and J. M. Williams, *J. Am. Chem. Soc.*, 1981, **103**, 5517–5522. (b) B. R. James, D. Mahajan, S. J. Rettig and G. M. Williams, *Organometallics*, 1983, **2**, 1452–1458. (c) L. Zamostna, S. Sander, T. Braun, R. Laubenstein, B. Braun, R. Herrmann and P. Klaring, *Dalton Trans.*, 2015, **44**, 9450–9469. (d) P. Singh, C. B. Dammann and D. J. Hodgson, *Inorg. Chem.*, 1973, **12**, 1335–1339. (e) M. Okazaki, A. Hayashi, C.-F. Fu, S.-T. Liu and F. Ozawa, *Organometallics*, 2009, **28**, 902–908.
30 (a) W. Scherer, A. C. Dunbar, J. E. Barquera-Lozada, D. Schmitz, G. Eickerling, D. Kratzert, D. Stalke, A. Lanza, P. Macchi, N. P. M. Casati, J. Ebad-Allah, and C. Kuntscher, *Angew. Chem., Int. Ed.*, 2015, **54**, 2505–2509. (b) M. Brookhart, M. L. H. Green and G. Parkin, *Proc. Natl. Acad. Sci.* 2007, **104**, 6908-6914. (c) W. Yao, O. Eisenstein and R. H. Crabtree, *Inorg. Chim. Acta*, 1997, **254**, 105-111.
31 H. A. Fargher, T. J. Sherbow, M. M. Haley, D. W. Johnson and Michael D. Pluth, *Chem. Soc. Rev.*, 2022, **51**, 1454–1469.
32 D. Evans, G. Yagupsky and G. Wilkinson, *J. Chem. Soc. A.*, 1968, 2660–2665.
33 Whilst $[IrH(CS)(PPh_3)_3]$ has been described previously, the corresponding rhodium complex has yet to be reported. (a) M. Yagupsky and G. Wilkinson, *J . Chem. Soc. A.*, 1968, 2813–2817. (b) W. R. Roper and K. G. Town, *J. Chem. Soc., Chem. Commun.,* 1977, 781–782.
34 K. Saikia, B. Deb and D. K. Dutta, *J. Mol. Cat. A.,* 2014, **381**, 188–193.
35 L. Hintermann, M. Perseghini, P. Barbaro and A. Togni, *Eur. J. Inorg. Chem.*, 2003, 601–609.
36 D. A. Valyaev, O. A. Filippov, N. Lugan, G. Lavigne and N. A. Ustynyuk, *Angew. Chem., Int. Ed.,* 2015, **54**, 6315-6319.
37 A. Plikhta, A. Pothig, E. Herdtweck and B. Rieger, *Inorg. Chem.*, 2015, **54**, 9517-9528.
38 (a) K. J. Harlow and A. F. Hill unpublished results. (b) K. J. Harlow, PhD Thesis, Imperial College London, 1998. (c) M. J. Doyle, M. F. Lappert, P. L. Pye and P. Terreros, *Dalton Trans.,* 1984, 2355-2364.
39 Ž. Selaković, A. M. Nikolić, V. Ajdačić and I. M. Opsenica, *Eur. J. Org. Chem.* **2022**, e202101265.
40 (a) J. Tsuji and K. Ohno*, Tetrahedron Lett.* 1965, **6**, 3969–3971. (b) D. H. Doughty and L. H. Pignolet, *J. Am. Chem. Soc.*, 1978, **100**, 7083–7085. (c) M. Kreis, A. Palmelund, L. Bunch and R. Madsen, *Adv. Synth. Catal.,* 2006, **348**, 2148–2154. (d) P. Fristrup, M. Kreis, A. Palmelund, P.-O. Norrby, R. Madsen, *J. Am. Chem. Soc.*, 2008, **130**, 5206–5215.
41 A. R. Sanger, *J. Chem. Soc., Dalton Trans.*, 1977, 120–129.
42 (a) R. D. Dewhurst, A. F. Hill, A. D. Rae, A. C. Willis, *Organometallics* 2005, **24**, 4703–4706. (b) A. F. Hill, A. D. Rae, M. Schultz, *Organometallics* 2007, **26**, 1325–1338.
43 B. Leforestier, M. R. Guton and A. B. Chaplin, *Angew. Chem., Int. Ed.,* 2020, **59**, 23500–23504.
44 (a) O. Gevert, J. Wolf and H. Werner, *Organometallics,* 1996, **15**, 2806-2809. (b) J. Gil-Rubio, M. Laubender and H. Werner, *Organometallics*, 1998, **17**, 1202–1207.

Table of Contents Text

A range of bimetallic rhodium species undergo double aminal CH activation to afford κ^3-*P,C,P'*-NHC pincer complexes based on economically accessible pro-ligands.

Table of Contents Graphic